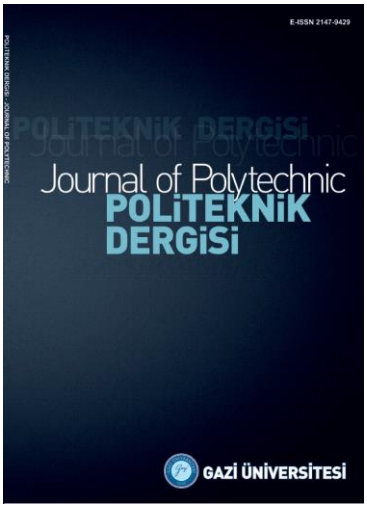


**POLİTEKNİK DERGİSİ**

***JOURNAL of POLYTECHNIC***

ISSN: 1302-0900 (PRINT), ISSN: 2147-9429 (ONLINE)
URL: http://dergipark.gov.tr/politeknik


# Investigation of Hardox 400 Steel exposed to heat treatment processes in WEDM

*Yazar (Author): Mehmet ALTUĞ*

*ORCID: 0000-0002-4745-9164*

**Bu makaleye şu şekilde atıfta bulunabilirsiniz(To cite to this article)**: Altuğ M.“ Investigation of Hardox 400 Steel exposed to heat treatment processes in WEDM”, ***Politeknik Dergisi***, 22(1): 237-244, (2019).

**Erişim linki (To link to this article):** http://dergipark.gov.tr/politeknik/archive

**DOI:** **10.2339/politeknik.417764**

# Investigation of Hardox 400 Steel Exposed to Heat Treatment Processes in WEDM

*Araştırma Makalesi / Research Article*

**Mehmet ALTUĞ***

*Malatya Meslek Yüksek Okulu, Makine ve Metal Tek. Bölümü, İnönü Üniversitesi, Türkiye

(Geliş/Received : 05.02.2018 ; Kabul/Accepted : 08.03.2018)

**ABSTRACT**

In this study, microstructure, mechanical, and conductivity characteristics of Hardox 400 steel were changed with different heat treatments and effect of such characteristics on its machinability with Wire Electrical Discharge Machining (WEDM). Optical microscope examinations were performed to determine various characteristics, and additionally microhardness and conductivity measurements were conducted hereof. L18 Taquchi test design was conducted with three levels and four different parameters to determine the effect of such alterations on its machinability with WEDM and post-processing Cutting width (kerf), Surface roughness (Ra), Material removal rate (MRR) values were determined. Micro changes were ensured successfully by using applied heat treatments. The best kerf value was obtained from sample 6 which was tempered from 350 °C. The microstructure of this sample was composed of commonly α ferrite and few pearlites. The best Ra value was obtained from sample 3 which was tempered from 200 °C. The microstructure of this sample was composed of few α ferrite and commonly pearlites. The best MRR value was obtained from sample 5 which was tempered from 300 °C. The microstructure of this sample was composed of almost equally α ferrite and pearlites. Additionally the most effective parameters on Ra were determined as hardox and current. The most effective parameters on kerf and MRR were determined as time off and hardox.

**Keywords: Hardox steel, heat treatment, microstructure, WEDM, kerf, Ra, MRR.**

## 1. INTRODUCTION

WEDM is one of non-traditional processes which are accepted globally to machine high strength-to-weight ratio materials mainly in industries. WEDM has numerous applications in aerospace, tool, mold, automotive, and medical industries to produce complex and intricate shapes. Due to ability to make intricate shape and machining of hard material with WEDM, it was observed that it increased. WEDM has capability to machine any kind of electrically conductive work in the present day. The most important machining responses of the process are the material removal rate, the roughness of the machined surfaces, and the kerf, which is the effective width of cut [1-4]. Kerf, Ra, MRR are expressed as the cutting width in the WEDM processes. Cutting mechanism in WEDM bench are shown in Fig.1. This depends on machining parameters as current, time off, wire speed, wire tension.

Some studies were conducted in order to determine important machining parameters for performance measures like MRR, surface finish and kerf in the WEDM process. Factors such as discharge current, pulse duration, and dielectric flow rate and their interactions have been found to play a significant role in rough cutting operations for maximization of MRR, minimization of surface roughness and minimization of cutting width by using Taguchi's experimental design method [5-8].

Some important studies has also been done on the machinability of steels in WEDM (9-11). In addition, important study has been done to optimize the WEDM parameters (12-19). While there is much studies with the weldability of hardox steels (20-21), there are very few studies on machinability. Some of these studies are related to waterjet (22,23) and laser plasma and plasma cutting (24-28).

Considering the studies published on WEDM; processing parameters and designated change of processing performance outputs such as kerf, Ra, MRR, and metallurgical structure change were analyzed by several studies. Detailed literature review conducted has showed that number of studies examining kerf characteristics of work piece based on metallurgical structure and microhardness change by using Hardox steel is limited and studies published in a limited number have not been comprehensive. In this regard, experimental and theoretical studies would a great contribution to this field. For this reason, this study investigated effects of microhardness, microstructure and conductivity of the sample with WEDM parameters- current, time off, wire speed and wire tension- and revealed effect of interaction of feature-parameter with kerf, Ra and MRR.

## 2. MATERIAL and METHOD

Microstructures, microhardness, and electric conductivity of samples of Hardox Steel exposed to heat treatments under different conditions were examined in this study. The purpose of this study is to obtain a distinct change on the sample micro structures by applying heat treatment and to determine the effect of these changed microstructures on machinibility with WEDM. The sizes of kerf, Ra and MRR were measured with Taguchi experimental design by cutting them in the wire bench as specified by the experimental study. The S/N ratio, one-

*Sorumlu yazar (Corresponding Author)
e-posta: mehmet.altug@inonu.edu.tr

way analysis of variance, and 3D graphics were examined by using Minitab 14 program. Heat treatments specified in Table 1 were applied to Hardox Steel, chemical compound of which is present in Table 2, mechanical properties of which is present in Table 3 under normal atmosphere conditions. These samples exposed to heat treatment were processed with WEDM by using the parameters in Table 4. In order to determine the sample features, which were changing as a result of heat treatment; microhardness, optical microscope in Nikon device, microstructure, mechanical features and conductivity to machinability with WEDM were investigated.

**Table 4.** Parameters and Levels

| | Parameters | Levels | | | | | |
|---|---|---|---|---|---|---|---|
| | | I | II | III | IV | V | VI |
| a | Heat treated samples | 1(A) | 2(B) | 3(C) | 4(D) | 5(E) | 6(F |
| b | Current (Amp) | 4 | 5 | 6 | | | |
| c | Time off (µs) | 100 | 150 | 225 | | | |
| d | Wire feed (m/min) | 4 | 6 | 9 | | | |
| e | Wire Tension (g) | 12 | 15 | 18 | | | |

**Table 1.** Heat treatments applied to Hardox Steel plates

| Sample | Heat treatment |
|---|---|
| **1** | Heating to 940 °C (20 minute) holding and quenching |
| **2** | Heating to 940 °C (20 minute) holding and quenching + Heating to 150°C and holding 2 h after air cooling |
| **3** | Heating to 940 °C (20 minute) holding and quenching + Heating to 200°C and holding 2 h after air cooling |
| **4** | Heating to 940 °C (20 minute) holding and quenching + Heating to 250°C and holding 2 h after air cooling |
| **5** | Heating to 940 °C (20 minute) holding and quenching + Heating to 300°C and holding 2 h after air cooling |
| **6** | Heating to 940 °C (20 minute) holding and quenching + Heating to 350°C and holding 2 h after air cooling |

**Table 2.** Chemical composition of Hardox Steel

| Element | C | Si | Mn | P | S | Cr | Ni | Mo | B |
|---|---|---|---|---|---|---|---|---|---|
| [wt. %] | 0,32 | 0,70 | 1,60 | 0,025 | 0,010 | 2,50 | 1,50 | 0,60 | 0,004 |

**Table 3.** Mechanical properties of Hardox Steel

| Tensile strength | Yield strength | Impact energy [J] | Hardness [HB] | Elongation [%] |
|---|---|---|---|---|
| 1080 | 900-1100 | 45 | 370-430 | 8 |

Experimental trials were carried out in a AF 250 high precision CNC WEDM. The experimental setup was as follows: Zinc coated brass wire with 0.25 mm diameter was employed as an electrode, and dimensions of Hardox steel samples were 5 mm x 50 mm x 100 mm in all the experiments. The behavior of six control factors as heat treated samples, current, time off, wire speed and wire tension was examined in this study. Table 4 illustrates control factors and their levels with symbols. The kerf value was measured by using LEICA DM4000M optical microscope device. While the control factors were used to select the best conditions for stability in the design of manufacturing process, the noise factors referred to all factors that cause variation. The experimental observations were further converted into a signal-to-noise (S/N) ratio by using Eq. (1) and Eq. (2). The signal-to-noise (S/N) ratio for "Larger is better" and "Smaller is better" were calculated as follows [29];

Larger is better;

$$S/N_L = -10\log\left(\frac{1}{n}\sum_{i=1}^{n}\frac{1}{y_i^2}\right) \quad (1)$$

Smaller is better;

$$S/N_S = -10\log\left(\frac{1}{n}\sum_{i=1}^{n}y_i^2\right) \quad (2)$$

## 3. RESULTS AND DISCUSSION

### 3.1 Optical microscope

In this study, commercial item microstructure having no heat treatment has tempered martensite phase structure (Fig.2). These steels are produced fully hardened and supplied to the market [20,30]. In Fig. 3(a), microstructure quenched at 940 $^{o}$C is shown (Sample 1). This microstructure was seen to have martensite phase structure. In Fig. 3(b) material microstructure tempered at 150 $^{o}$C is seen (Sample 2). This microstructure consists of tempered martensite and fine α-ferrit phases and was formed at the α-ferrite phase boundaries. After quenching it was observed that the amount of α-ferrite increased in the tempered material microstructure at 200 $^{o}$C (Sample 3) and the martensite phase structure was converted to pearlite (Fig 3(c)). It was also seen that the pearlite lamellas were surrounded by α-ferrite phase. In Figures 3(d) and (e) microstructures of tempered samples at 250 $^{o}$C (Sample 4) and 300 $^{o}$C (Sample 5) are given respectively. In these microstructures as the tempering temperature increased α-ferrite phase volume also increased whereas pearlite phase volume decreased. In Fig. 3(f) , in the sample microstructure tempered at 350 $^{o}$C (Sample 6), pearlite phase was observed at the α-ferrite grain boundaries. It was determined that α-ferrite phase was more dominant in this microstructure.

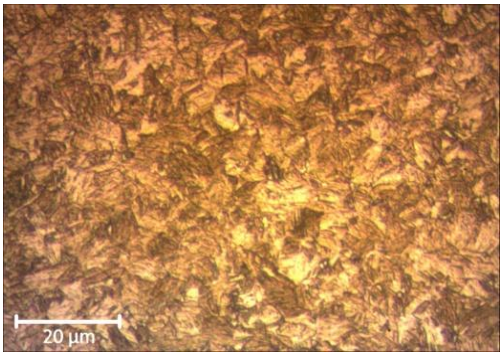


**Fig. 2.** The optical microscope images of the Hardox 400

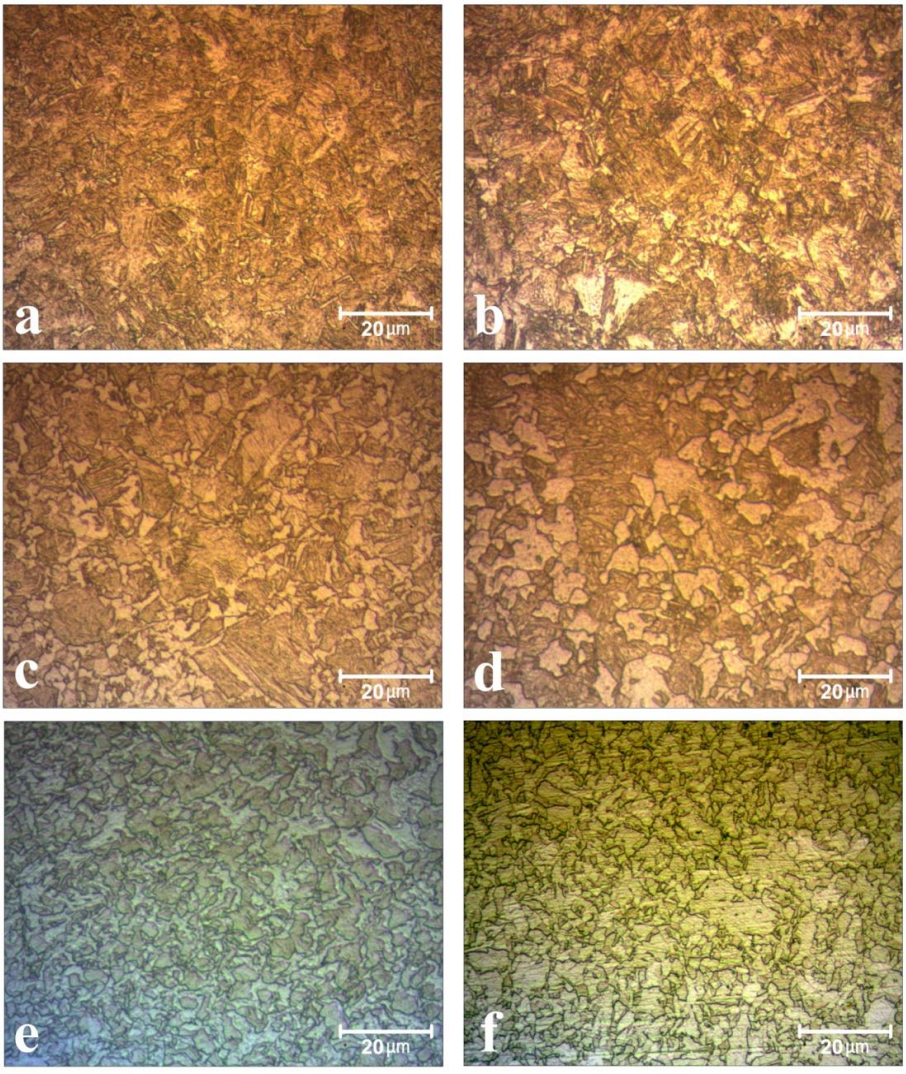


**Fig.3.** The optical microscope images of the samples

### 3.2 Micro Hardness

In Fig. 4, hardness results were given with a graph. Hardness value was 386 HV after quenching at 950ºC. After tempering heat treatment hardness decreased. Hardness values of the samples tempered at 200 C and 250 C increased (even if in small amount) compared to hardness of samples tempered at 150 ºC. This increase is attributed to carbides formed during tempering. It was specified that hardness of samples tempered at 300 and 350 ºC decreased inversely proportional with the increasing tempering temperature . As the tempering temperature increased, decrease in the hardness values of the samples increased too.

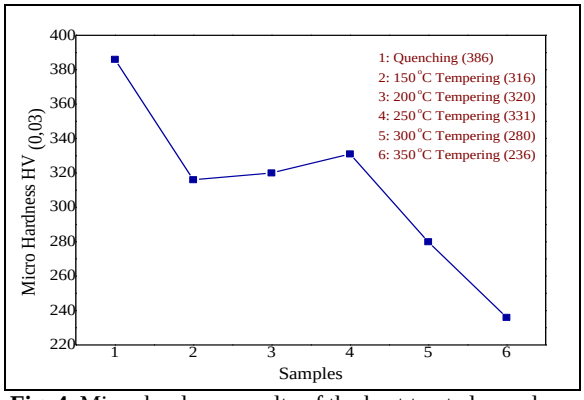


**Fig. 4.** Micro hardness results of the heat treated samples

### 3.3 Resistivity And Conductivity

Electrical conductivities of the heat treated samples are given in Fig. 5. As it is seen from the graph, electrical conductivity of the quenched sample came out to be lower than that of tempered samples (except the sample tempered at 200ºC). Electrical resistance of the stressed structure created as the result of quenching was high. Conductivity of the sample tempered at 150ºC increased. It is thought that this conductivity increase is because of settling of Carbon atoms to unstable position after quenching and then to more stable positions during tempering with decreasing stressed structure. Conductivity of the sample tempered at 200ºC hand an increase was found in the sample conductivity tempered at 250ºC. It is thought that this increase is due to diffusion of the carbides to low strained areas. Conductivity increased as the tempering temperature (300ºC and 350ºC) increased. This increase can be attributed to increasing α-ferrite phase volume and decreasing pearlite phase volume.

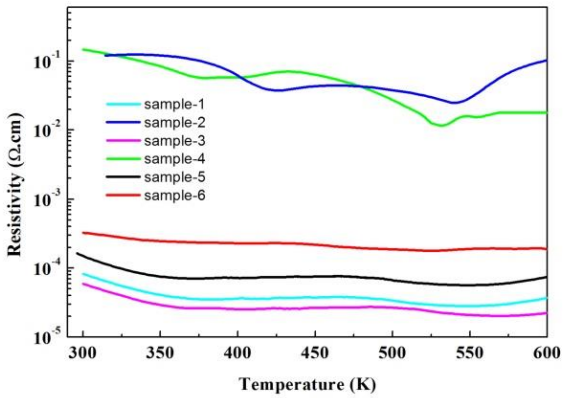


**Fig. 5.** The resistivity results of the heat treated samples

### 3.4 Kerf (Cutting Width)

At the end of the tests made in wire erosion (WEDM), the obtained values of kerf, surface roughness (Ra) and material removal rate (MRR) and S/N ratios obtained after Taguchi analysis are given in Table 5.

According to Fig.6, the lowest kerf values were obtained with the 6, 2 and 4 numbered samples respectively. The sample 6 was tempered at high temperature and therefore had the lowest hardness value. For this reason the best kerf result can be attributed to the decrease in hardness. The second best kerf value was obtained on the number 2 sample. Conductivity of sample 2 was higher with

| Exp. No | Parameters | | | | | Kerf (µ) | | Ra (µm) | | MRR (g.min$^{-1}$) | |
|---|---|---|---|---|---|---|---|---|---|---|---|
| | a | b | c | d | e | Result | S/N | Result | S/N | Result | S/N |
| 1 | 1 | 4 | 100 | 4 | 12 | 238 | -47,531 | 3,08 | -9,771 | 0,308 | -10,229 |
| 2 | 1 | 5 | 150 | 6 | 15 | 244 | -47,747 | 2,97 | -9,455 | 0,289 | -10,782 |
| 3 | 1 | 6 | 225 | 9 | 18 | 255 | -48,130 | 2,81 | -8,974 | 0,268 | -11,437 |
| 4 | 2 | 4 | 100 | 6 | 15 | 239 | -47,568 | 2,98 | -9,484 | 0,287 | -10,842 |
| 5 | 2 | 5 | 150 | 9 | 18 | 245 | -47,783 | 2,91 | -9,277 | 0,268 | -11,437 |
| 6 | 2 | 6 | 225 | 4 | 12 | 248 | -47,889 | 2,91 | -9,277 | 0,275 | -11,213 |
| 7 | 3 | 4 | 150 | 4 | 18 | 245 | -47,783 | 2,86 | -9,157 | 0,299 | -10,486 |
| 8 | 3 | 5 | 225 | 6 | 12 | 249 | -47,924 | 2,89 | -9,217 | 0,288 | -10,812 |
| 9 | 3 | 6 | 100 | 9 | 15 | 245 | -47,783 | 2,85 | -9,127 | 0,279 | -11,087 |
| 10 | 4 | 4 | 225 | 9 | 15 | 250 | -47,958 | 2,91 | -9,277 | 0,262 | -11,634 |
| 11 | 4 | 5 | 100 | 4 | 18 | 241 | -47,640 | 2,98 | -9,484 | 0,293 | -10,662 |
| 12 | 4 | 6 | 150 | 6 | 12 | 244 | -47,747 | 2,93 | -9,337 | 0,280 | -11,056 |
| 13 | 5 | 4 | 150 | 9 | 12 | 246 | -47,818 | 2,97 | -9,455 | 0,299 | -10,486 |
| 14 | 5 | 5 | 225 | 4 | 15 | 251 | -47,993 | 3,02 | -9,600 | 0,291 | -10,722 |
| 15 | 5 | 6 | 100 | 6 | 18 | 246 | -47,818 | 2,95 | -9,396 | 0,288 | -10,812 |
| 16 | 6 | 4 | 225 | 6 | 18 | 249 | -47,924 | 2,89 | -9,187 | 0,271 | -11,340 |
| 17 | 6 | 5 | 100 | 9 | 12 | 239 | -47,568 | 2,98 | -9,455 | 0,293 | -10,662 |
| 18 | 6 | 6 | 150 | 4 | 15 | 241 | -47,640 | 2,90 | -9,217 | 0,281 | -11,025 |

**Table 5.** Taguchi $L_{18}$ orthogonal array, experimental results

decreased. A partial increase was determined in the hardness of this sample. The increase in hardness was thought to be because of carbide formation, similarly the decrease of conductivity in the same sample can be attributed to the formation of these carbides. On the other

respect to other samples. The increase in sample conductivity decreased the kerf value. The third best kerf value was obtained with the sample 4. The conductivity of this sample had the second best conductivity value. The positive effect of higher conductivity to kerf values was also determined on this sample. It was already stated that the change in hardness and conductivity values was due to the microstructural variation. An increase was observed in the kerf values with the increasing time off values. Similar results were also observed in some studies in literature [1,10,15].

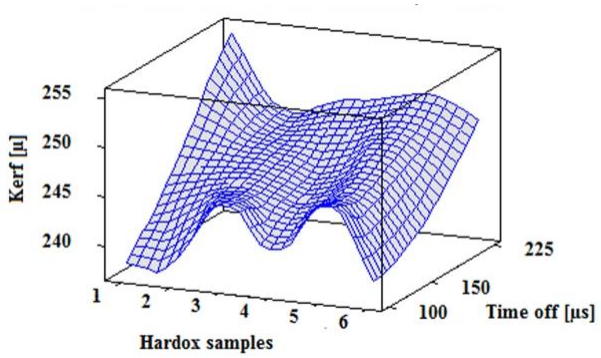


**Fig. 6.** Effect of the Heat treated Hardox and Time off on kerf

When the Fig. 7 was examined a general increase was observed in the kerf values depending on the increasing wire feed and wire tension values. There are similar results in some studies in literature [12].

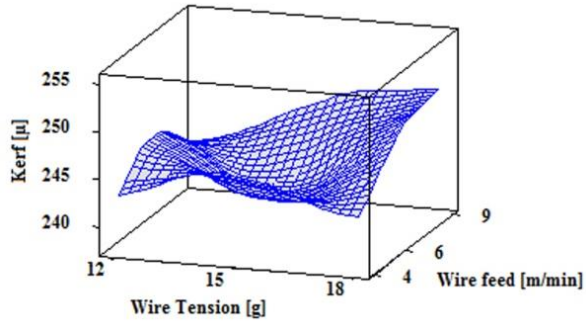


**Fig. 7.** Effect of the wire tension and wire feed on kerf

Effects of current on the kerf values of samples are given in Fig. 8. İncrease in the current values caused a significant amount of increase on the kerf values. Some studies in literature have parallel results.

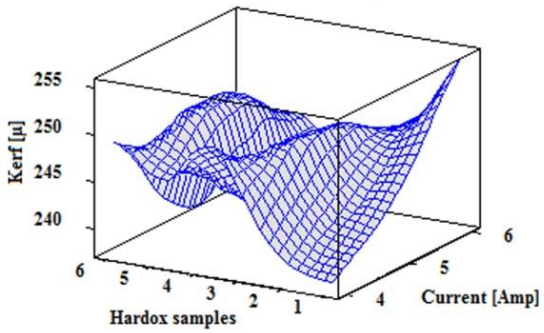


**Fig. 8.** Effect of the Heat treated Hardox and Current on kerf

ANOVA analysis with which the effects of parameters on kerf were examined is given in Table 6. According to the table all of the parameters are significantly effective on kerf. Difference in the kerf values of hardox samples after heat treatment shows the accuracy and the contributions of the applied heat treatment.

**Table 6.** Result of ANOVA for Kerf

| Source | DF | SS | MS | F | P | % |
|---|---|---|---|---|---|---|
| **Hardox** | 5 | 41,611 | 8,322 | 17,62 | 0,008 | 11,1 |
| **Current** | 2 | 13,778 | 6,889 | 14,59 | 0,015 | 3,6 |
| **Time off** | 2 | 254,111 | 127,056 | 269,06 | 0,000 | 70,6 |
| **Wire feed** | 2 | 21,444 | 10,722 | 22,71 | 0,007 | 5,7 |
| **Wire tension** | 2 | 24,778 | 12,389 | 26,24 | 0,005 | 6,7 |
| **Error** | 4 | 1,889 | 0,472 | | | |
| **Total** | 17 | 357,611 | | | | |

### 3.5 Surface Roughness (Ra)

According to Fig. 9 lower Ra values were obtained with 3, 6 and 2 numbered samples. The main reason of this difference is thought to be the variations in the hardness and conductivity values after heat treatment. In this regard, since the highest resistance was with the number 3 sample ,the surface roughness value came out to be the lowest. A decrease (even if a small amount) was observed in Ra values with the increasing time off values. However, in some studies in literature, Ra values increased depending on the increase of gap period between two pulses [12,13].

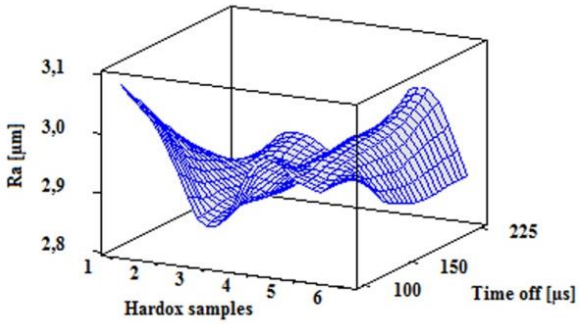


**Fig. 9.** Effect of the Heat treated Hardox and Time off on Ra

From Fig. 10 a general decrease was observed in the Ra values depending on the increasing wire feed and wire tension values. Similar results were also encountered in literature [12,13].

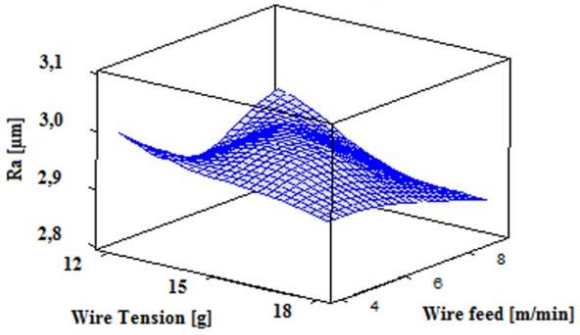


**Fig. 10.** Effect of the wire tension and wire feed on Ra

Effects of current on the Ra values in the samples are given in Fig.11. Increase in the current values caused a significant decrease in the Ra values as also seen in literature . [12,13,14].

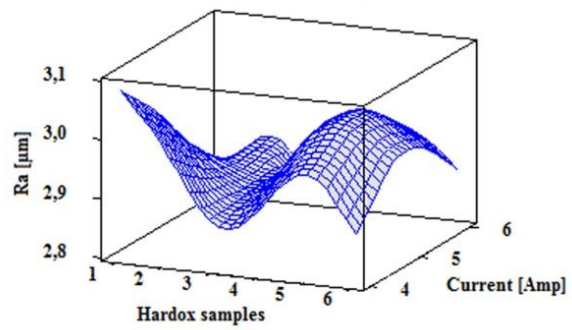


**Fig. 11.** Effect of the Heat treated Hardox and Current on Ra

ANOVA analysis where the effects of parameters were examined on Ra is given in Table 7. According to the Table , wire feed values had no significant effects on Ra but all the other parameters were effective on Ra.

**Table 7.** Result of ANOVA for Ra

| Source | DF | SS | MS | F | P | % |
|---|---|---|---|---|---|---|
| **Hardox** | 5 | 0,0198 | 0,00396 | 6,29 | 0,049 | 25,6 |
| **Current** | 2 | 0,0150 | 0,00750 | 11,9 | 0,021 | 19,9 |
| **Time off** | 2 | 0,0140 | 0,00702 | 11,1 | 0,023 | 16,8 |
| **Wire feed** | 2 | 0,0085 | 0,00427 | 6,78 | 0,052 | 10,1 |
| **Wire tension** | 2 | 0,0105 | 0,00527 | 8,36 | 0,037 | 13,7 |
| **Error** | 4 | 0,0025 | 0,00063 | | | |
| **Total** | 17 | 0,0705 | | | | |

### 3.6 Material removal rate (MRR)

From the Fig. 12 it is seen that higher MRR values were obtained with 5, 3 and 1 numbered samples. It is thought that the root cause of this distinctness is the variations in the hardness and conductivity values after heat treatment. MRR and kerf results were in conformity with each other. Because the highest kerf value was obtained with the number 5 sample. Therefore the highest MRR value was also obtained with the number 5 sample. A decrease was also observed in MRR values with increasing time off values as seen in some steel studies in literature [17,18,19].

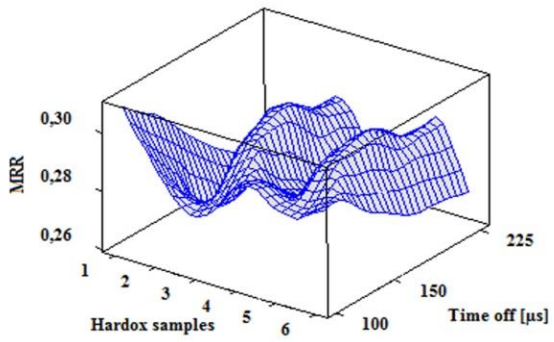


**Fig. 12.** Effect of the Heat treated Hardox and Time off on MRR

According to Fig. 13 a general decrease was seen in MRR values depending on the increasing wire feed and wire tension values as seen in literature [5,12,17].

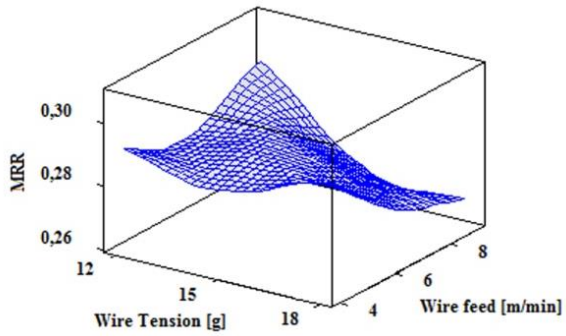


**Fig. 13.** Effect of the wire tension and wire feed on MRR

Effects of current on the MRR values in the samples are given in Fig. 14. Here, the increase in the current values caused a decrease (even if in small amount) in the MRR values. In literature some studies consist similar results [6,16].

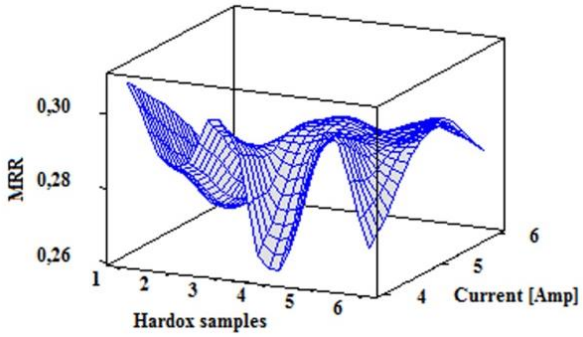


**Fig. 14.** Effect of the Heat treated Hardox and Current on MRR

ANOVA analysis where the effects of parameters on MRR were examined is given in Table 8. According to the Table, all of the parameters were significantly effective on MRR.

**Table 8.** Result of ANOVA for MRR

| Source | DF | SS | MS | F | P | % |
|---|---|---|---|---|---|---|
| **Hardox** | 5 | 0,000618 | 0,000124 | 6,66 | 0,045 | 19,9 |
| **Current** | 2 | 0,000313 | 0,000157 | 8,45 | 0,037 | 9,9 |
| **Time off** | 2 | 0,000744 | 0,000372 | 20,05 | 0,008 | 27,3 |
| **Wire feed** | 2 | 0,0005 | 0,000255 | 13,74 | 0,016 | 18,2 |
| **Wire** | 2 | 0,000336 | 0,000168 | 9,07 | 0,033 | 11,2 |
| **Error** | 4 | 0,000074 | 0,000019 | | | |
| **Total** | 17 | 0,002596 | | | | |

## 4. CONCLUSION

Different heat treatments were carried out to the samples of Hardox 400 used in the industry and their microstructure, microhardness and conductivity characteristics were changed. Effect of this characteristic change on machinability with WEDM was investigated with Taguchi method and ANOVA. S/N ratio of these results was determined.

- The lowest hardness value was obtained in the tempered sample-6 whereas the highest hardness value was obtained in the sample-1 which was water quenched from austenite. It was determined that microstructure of this sample has martensitic phase. When martensitic phase was tempered (in the sample 2), decrease was observed in hardness. The microhardness values of sample 3 and 4 were a slightly increased due to carbides which occurred in the microstructure with tempered. When the tempering temperature increased, the microhardness values of sample 5 and 6 decreased.
- The most effective parameters on Ra were determined as hardox and current. The most effective parameters on Kerf and MRR were determined as time off and hardox.
- The microhardness value of sample 6 was lower than the microhardness values of other samples. Therefore the kerf value of sample 6 was the best. The lowest microhardness could attribute to this result.
- In sample (2) having a tempered (150 $^{o}$C) martensite structure with the best conductivity, it was seen in (3) sample of having a tempered (200 $^{o}$C) in the lowest conductivity.
- Kerf, Ra and MRR values, obtained according to the experimental design by using the taguchi experimental design method in the experimental studies, were converted to S/N ratios and the best parameter levels were determined. By using analysis of variance (ANOVA),
- Average best surface roughness (Ra) values after processing with WEDM were obtained in the ranking of 3, 6, 2, 4, 1 and 5. According to these results, it was determined that best and worst surface roughness values were obtained from tempered martensite structures (200 $^{o}$C) and tempered martensite structures (300 $^{o}$C), respectively.
- Average best MRR values after processing with WEDM were obtained in the ranking of 5, 3, 1, 6, 4 and 2. According to these results, it was determined that best and worst MRR values were obtained from tempered martensite structures (300 $^{o}$C) and tempered martensite structures, tempered martensite structures (150 $^{o}$C), respectively.
- The best (lowest) kerf value was obtained from sample-6 that was tempered from 350 $^{o}$C. The microstructure of this sample was composed of commonly α-ferrite and few pearlites. The worst (highest) kerf value was obtained from sample-5. This sample had tempered martensite microstructure. In other words, the microstructure of this sample was composed of α-ferrite and pearlite. The electricity conductivity of the sample 5 had the worst than the electricity conductivity of the sample 6. Therefore,as the conductivity capacity of sample decreased, the kerf value increased.
- The best (lowest) Ra value was obtained from sample-3 that was tempered from 200 $^{o}$C. The microstructure of this sample was composed of few α-ferrite and commonly pearlites. This sample had the lowest electricity conductivity, therefore the best Ra value could attribute to this result.
- The best MRR value was obtained from sample-5 that was water quenching from 300 $^{o}$C. The microstructure of this sample was composed of almost equally α ferrite and pearlites. The worst MRR value was obtained from sample-2. The microstructure of this sample was composed of martenzite and fine α-ferrite. It was observed that, MRR and kerf values of this sample comfirmed each other.

## ACKNOWLEDGEMENTS

This study is supported by Inonu University Scientific Researches Projects. Thank to the Rectorate of Inonu University for their support. Thank you for your contributions to "Çetin Cıvata" and "Turgut Durmaz".

## REFERENCES

[1] Aqueel S., Mufti N.A., Rakwal D., Bamberg E., "Material Removal Rate, Kerf, and Surface Roughness of Tungsten Carbide Machined with Wire Electrical Discharge Machining", ***Journal of Materials Engineering and Performance***, 20(1): 71-76, (2011).

[2] Yan M.T., Huang P.H., "Accuracy Improvement of WireEDM by Real-Time Wire Tension Control", ***Int. J. Mach. Tools Manuf.***, 44(7–8): 807-814, (2004).

[3] Hsue A.W.J., Su H.C., "Removal Analysis of WEDM Tapering Process and Its Application to Generation of Precise Conjugate Surface", ***Journal of Materials Processing Technology***, 149(1-3): 117-123, (2004).

[4] Rakwal D., Bamberg E., "Slicing, Cleaning and Kerf Analysis of Germanium Wafers Machined by Wire Electrical Discharge Machining", ***Journal of materials processing technology***, 209(8): 3740-3751, (2009).

[5] Mahapatra S.S., Patnaik A., "Optimization of wire electrical discharge machining (WEDM) process parameters using Taguchi method", ***International Journal of Advanced Manufacturing Technology***, 34(9-10): 911-925, (2007).

[6] Jangra K., Jain A., Grover S., "Optimization of multiple-machining characteristics in wire electrical discharge machining of punching die using grey relational analysis", ***Journal of Scientific and Industrial Research***, 69: 606-612, (2010).

[7] Hari S., Khanna R., "Parametric optimization of Cryogenic treated D-3 for cutting rate in wire electrical discharge machining", ***J Eng. Technology***, 1:(2) 59–64, (2011).

[8] Kansal H.K., Singh S., Kumar P., "Parametric optimization of powder mixed electricaldischarge machining by response surface methodology", ***Journal of Materials ProcessingTechnology***, 169(3): 427-436, (2005).

[9] Gupta P., Khanna R., Gupta R.D., Sharma N., "Effect of process parameters on kerf width in WEDM for HSLA using response surface methodology", ***Journal of Engineering and Technology***, 2(1): 1-6, (2012).

[10] Tosun N., Cogun C., Tosun G., "A study on kerf and materials removal rate in wire electrical discharge machining based on taguchi method", ***Journal of Materials Processing Technology***, 152: 316-322, (2004).

[11] Chaudhary R., Rampal R., Sharma N., "Investigation and Optimization of Material Removal Rate For Wire Cut Electro Discharge Machining In EN5 Steel Using Response Surface Methodology", ***International Journal of Latest Trends in Engineering and Technology***, 3(1): 192-199, (2013).

[12] Altuğ M., Erdem M., Ozay C., "Experimental investigation of kerf of Ti6Al4V exposed to different heat treatment processes in WEDM and optimization of parameters using genetic algorithm", ***International Journal of Advanced Manufacturing Technology***, 78: 1573-1583, (2015).

[13] Kuriakose S., Shunmugam M.S., "Multi-objective optimization of wire electro-discharge machining process by Non-dominated Sorting Genetic Algorithm", ***Journal of Materials Processing Technology***, 170: 133-141, (2005).

[14] Pasam V.K., Battula S.B., Madar V.P., Swapna M., "Optimizing Surface Finish in WEDM Using the Taguchi Parameter Design Method", ***Journal of the Brazilian Society of Mechanical Sciences and Engineering***, XXXII(2): 107-113, (2010).

[15] Ikram A., Mufti N.A., Saleem M.Q., Khan A.R., "Parametric optimization for surface roughness kerf and MRR in wire electrical discharge machining (WEDM) using Taguchi design of experiment", ***Journal of Mechanical Science and Technology***, 27(7): 2133-2141, (2013).

[16] Jabbaripour B., Sadeghi M.H., Faridvand S.H., Shabgard M. R., "Investigating the effects of edm parameters on surface integrity MRR and TWR in machining of Ti-6Al-4V", ***Machining Science and Technology***, 16: 419-444, (2012).

[17] Singh J., Sharma S., "Effects of Process Parameters on Material Removal Rate and Surface Roughness in WEDM of H13 Tool Steel", ***International Journal of Current Engineering and Technology***, 3(5): 1852-1857, (2013).

[18] Shah A., Mufti N. A., Rakwal D., Bamberg E., "Material Removal Rate, Kerf, and Surface Roughness of Tungsten Carbide Machined with Wire Electrical Discharge Machining", ***Journal of Materials Engineering and Performance***, 20(1): 71-76, (2011).

[19] Bobbili R., Madhu V., Gogia A.K., "Effect of Wire-EDM Machining Parameters on Surface Roughness and Material Removal Rate of High Strength Armor Steel", ***Materials and Manufacturing Processes***, 28: 364-368, (2013).

[20] Frydman S., Konat L., Kalskı G., "Structure and hardness changes in welded joints of Hardox steels", ***Archives Civil and Mechanical Engineering***, VIII(4): 15-27, (2008).

[21] Konovalov S.V., et al., "Formation Wear Resistant Coatings on Martensite Steel Hardox 450 by Welding Methods", ***Materials Science and Engineering***, 142: 2-5, (2016).

[22] Filip A.C., et al., "Experimental research on the machinability of Hardox steel by abrasive waterjet cutting", ***DOI: 10.1051/matecconf/20179403003*** (2017).

[23] Hlavac L.M., et al., "Experimental method for the abrasive water jet cutting quality", ***Journal of Materials Processing Technology***, 209: 6190-6195, (2009).

[24] Chamarthia S., et al., "Investigation Analysis of Plasma arc cutting Parameters on the Unevenness surface of Hardox-400 material", ***Procedia Engineering***, 64: 854-861, (2013).

[25] Mindivan H., "Effects of Combined Diffusion Treatments on the Wear Behaviour of Hardox 400 Steel", ***Procedia Engineering***, 68: 710-715, (2013).

[26] Gondalia R.V., Sharma A.K., "Parametric Investigation and Optimization of Co2 Laser Cutting process used for Cutting Hardox-400 materials", ***International Journal of Science and Engineering Applications***, 2(6): 123-129, (2013).

[27] Prajapati B.D., Patel R.J., Khatri B.C., "Parametric Investigation of CO2 Laser Cutting of Mild Steel and Hardox-400 Material", ***International Journal of Emerging Technology and Advanced Engineering***, 3(4): 204-208, (2013).

[28] Majerik J., Barenyi I., "Experimental Investigation Into Tool Wear Of Cemented Carbide Cutting Inserts When Machining Wear Resistant Steel Hardox 500", ***Engineering Review,*** 36(2): 167-174, (2016).

[29] Montgomery D.C., "Design and Analysis of Experiments, Wiley, New York, USA, (2001).

[30] Gökmeşe H., Özdemir M., "The Effect Of Heat Treatment On The Formability Behavior Of Hardox-500 Sheet Material", ***Gazi University J. Sci Part:C***, 4(4): 343-349, (2016).